STEM CELLS AND DEVELOPMENT
Volume 21, Number 3, 2012

DOI: 10.1089/scd.2010.0513

Human Schwann Cells Retain Essential Phenotype Characteristics After Immortalization

Helmar C. Lehmann,[1,2] Weiran Chen,[1] Ruifa Mi,[1] Shuo Wang,[1] Ying Liu,[3] Mahendra Rao,[4] and Ahmet Höke[1]

Schwann cells (SCs) play an important role in the pathogenesis of peripheral nerve diseases and represent a potential target for development of therapies. However, use of primary human SCs (hSCs) for in vitro models is limited because these cells are difficult to prepare and maintain in high yield and purity under common cell culture conditions. To circumvent this obstacle, we immortalized primary human fetal SCs using the SV40 large T-antigen and human telomerase reverse transcriptase expression vectors. After cloning, selection, and purification, we evaluated several immortalized SC lines for their ability to express extracellular matrix (ECM) molecules and myelinate embryonic rat sensory axons. In addition, we established a gene expression profile and explored their sensitivity to oxidative stress in a simple in vitro assay. Immortalized hSC clones expressed common glial markers and a broad variety of growth factors, receptors, and ECM molecules as determined by immunocytochemistry, microarray, and quantitative reverse transcription–polymerase chain reaction. In neuron-SC co-cultures, these cells were able to myelinate rat dorsal root ganglia neurons, although their effectiveness was lower in comparison to primary rat SCs. In toxicity assays, immortalized hSCs remain susceptible to oxidative stress induced by H_2O_2. This study shows that, using specific immortalization techniques, it is possible to establish hSC lines that retain characteristics of typical primary hSCs. These cells are particularly useful for drug screening and studies aimed at disease mechanisms involving SCs.

Introduction

Schwann cells (SCs) are considered to be the most important cellular component for nerve fiber regeneration in the peripheral nervous system (PNS). They provide a microenvironment that favors neural regeneration by producing neurotrophic factors [1–4] or expressing components of the basal lamina [5] and neuroprotective glycoproteins [6]. Apart from secretion of trophic and neuroprotective factors, morphological modification of SCs that lead to axon ensheathment and eventual formation of myelin are prerequisite for optimal function of the PNS. Injury and subsequent loss of SCs contributes to the pathogenesis of a broad variety of hereditary, metabolic, and inflammatory disorders of the PNS [7–10]. Although SCs have been recognized to be a major target in the pathogenesis of those disorders, identification and development of drugs that protect SCs from injury and promote myelination has been largely unsatisfactory so far [11]. This is partially attributable to the fact that studies for myelination and drug screening in the PNS are based on animal models and/or rodent cell culture systems, which may be difficult to translate into the human diseases [12]. Thus, the use of human SCs (hSCs) would be undoubtedly advantageous; however, since primary adult hSCs can only be prepared from samples of single individuals, their utility is limited. Moreover, although some studies suggest that it is feasible [13–15], expansion and maintenance of hSCs in culture has been difficult, due to low division rate and potential overgrow of fibroblasts over time [16–18]. The same obstacles apply, in addition to ethical issues, for primary embryonic stem cell-derived hSCs. Thus, we sought to determine the feasibility of generating an immortalized hSCs line that (i) retain essential characteristics of primary SCs including the ability to myelinate axons, (ii) is easy to grow in large quantities, and (iii) suitable for drug-screening assays.

Materials and Methods

All experiments were carried out with the approval of the Institutional Review Board and Animal Care and Use Committee. Tissue culture supplies were obtained from Invitrogen unless noted otherwise.

[1]Departments of Neurology and Neuroscience, Johns Hopkins University School of Medicine, Baltimore, Maryland.
[2]Department of Neurology, Heinrich-Heine-University, Düsseldorf, Germany.
[3]Regenerative Medicine Research Group, Life Technologies, San Diego, California.
[4]Regenerative Medicine Research Group, Life Technologies, Frederick, Maryland.

Generation of immortalized human fetal SC lines

Construction of SV40 large T-antigen and hTERT expression vectors. The SV40 large T-antigen was cloned using the pZipSV776-1 plasmid construct (kindly provided by Dr. William C. Hahn, Harvard University) as previously described [3]. Oligonucleotide sequence for polymerase chain reaction (PCR) was 5′-CACCGCTTTGCAAAGATGGATAAAG (sense) and 5′-AATTGCATTCATTTTATG-TTTCA (antisense). After amplification in an Expend High Fidelity PCR System (Roche) the PCR product was cloned into the pENTR/D-TOPO vector by directional TA-cloning. The target SV40 large T-antigen gene was subsequently transferred into pLenti6.2/V5-Dest vector using Gateway technology (Invitrogen). In this vector, the SV-40 large T-antigen is under the control of Pcmv, whereas the blasticidin resistance gene, which served as selection marker, was under the control of Psv40. The human telomerase reverse transcriptase (hTERT) expression construct pBabe-hygro-hTERT (also a kind gift from William C. Hahn at Harvard University) was used to subclone the hTERT gene into the pLenti3.2/V5-Dest vector as described above. In the destination vector, the hTERT was under the control of Pcmv, and the selection marker, neomycin resistance gene, was under the control of Psv40. The expression plasmids were prepared and purified using Plasmid MIDI Kit (Qiagen) and suspended in distilled water for electroporation.

Human fetal SC culture. Human fetal SCs were isolated from fetuses with a mean gestational age of 60–80 days, with consent, from women undergoing elective termination of pregnancy and approval by the Johns Hopkins Institutional Review Board. The individual human fetal samples were kept separate during the isolation procedure and SC cultures were established from sciatic nerves using a modification of the Brockes method [19]. Briefly, dissected sciatic nerves were digested with 0.1% collagenase (Worthington) and 0.25% trypsin. After blocking of enzymatic digestion with Dulbecco's modified Eagle's medium containing 10% fetal bovine serum (FBS), cells were centrifuged and subsequently mechanically dissociated. After plating, cells were treated with 2 cycles of cytosine arabinoside (10 μM) to eliminate fibroblasts.

Transfection by electroporation into SCs and selection of clones. Fetal SCs were cultured in Neurobasal media (Neurobasal modified Eagle's medium [MEM] plus 10% FBS, 0.5uM glutamin, 2% glucose, 1×B27 supplement). After 3–7 days, cells were harvested by scraping, washed, and further resuspended in Opti-MEM in a concentration of $0.8–1.0\times10^6$ cells per 100 μL. Then, the cells were mixed with 5 μg of the pLenti6/V5-DEST plasmid carrying hTERT gene (pLenti6/hTERT) in 1.7 μL TE (pH 8.0) and 15 μg pLenti6/V5-DEST plasmid carrying SV40 large T-antigen gene (pLenti6/SV40) in 5 μL TE (pH 8.0). After transfer to a 0.2 cm Gene Pulser cuvette (Bio-Rad) cells were incubated for 5 min at room temperature and then pulsed with a Gene Pulser Xcell Electroporation System (Bio-Rad) at 850 μF×90 V. Next, 500 μL ice-chilled culture media (antibiotics free) was added to the cells, and after 5 min, cells were transferred into a 75 cm^2 (T75) culture flask. Transfected SCs were cultured in antibiotic-free Neurobasal media for 3–7 days until 70%–80% confluence, before electroporation was repeated up to 4 times with different amounts of pLenti6/hTERT and pLenti6/SV40. For the second electroporation, 10 μg pLenti6/hTERT (in 3.3 μL TE, pH 8.0) and 10 μg pLenti6/SV40 (in 3.3 μL TE, pH 8.0) were used, whereas 15 μg pLenti6/hTERT (in 5 μL TE, pH 8.0) and 5 μg pLenti6/SV40 (in 1.7 μL TE, pH 8.0) was used for the third electroporation. After the 4th electroporation with 20 μg pLenti6/hTERT (in 6.6 μL TE, pH 8.0) and 2 μg pLenti6/SV40 (in 0.6 μL TE, pH 8.0), cells from each cuvette were transferred into 3 T75 culture flasks and cultured in Neurobasal media containing 5 μg/mL blasticidin (Invitrogen) for 6–8 days. Blasticidin-resistant colonies were detached with 0.05% trypsin, isolated with glass capillary pipettes, and subsequently expanded in blasticidin-containing cell media.

Functional characterization of immortalized hSCs

Immunocytochemistry. For immunocytochemistry, cultured immortalized *hSCs* were fixed with 4% paraformaldehyde for 30 min. After washing and blocking with 10% normal horse serum in 0.1% Triton-X for 1 h, primary antibodies were added for 12 h at 4°C. The following antibodies were used: mouse antiglial fibrillary acidic protein (anti-GFAP), rabbit anti-S100β (both Sigma-Aldrich), mouse anti-p75 (Millipore), and mouse anti-myelin basic protein (MBP) (SMI-94, Sternberger monoclonals). Blocking solution without primary antibody was added for 12 h at 4°C as control. Antibody binding was detected by using fluorescently labeled secondary antibodies (Vector Laboratories) at 1:500 dilution and cell nuclei were counterstained with 4′,6-diamidino-2-phenylindole. Appropriate controls included omission of primary and secondary antibodies.

Quantitative reverse transcription–PCR. For quantification of mRNA expression levels, a semi-quantitative (q) PCR analysis was performed as previously described [12]. Briefly, total RNA was extracted from cells with Trizol (Invitrogen) and complementary cDNA was synthesized using a template of 1 μg total RNA and "Ready-to-Go You Prime First Strand" beads (Amersham Pharmacia) and random primers (Invitrogen). Measurements of mRNA levels were performed by real-time reverse transcription (RT)–PCR using DNA Engine Opticon 2 System (M.J. Research Inc.) and the relative amount of gene of interest was normalized to the mRNA amount of an internal control [GAPDH (glyceraldehyde 3-phosphate dehydrogenase)]. To avoid the possibility of amplifying contaminating genomic DNA, all of the primers for real-time RT–PCR were designed with an intron sequence inside the cDNA to be amplified; reactions were performed with appropriate negative control samples (template-free control samples); a uniform amplification of the products was rechecked by analyzing the melting curves of the amplified products (dissociation graphs); the melting temperature (Tm) was 57°C to 60°C; the probe Tm was at least 10°C higher than primer Tm; and gel electrophoresis was performed to confirm the correct size of the amplification and the absence of nonspecific bands. All primers were synthesized by Integrated DNA Technologies. The real-time PCR parameters and primer sequences are available upon request.

Bead array gene expression analysis. Total RNA was isolated from near-confluent cells using the Qiagen RNEasy kit (Qiagen, Inc.). A total amount of 100 ng total RNA was used for amplification by the method of van Gelder et al. [20]. An Illumina RNA Amplification kit (Ambion, Inc.) was used for RNA synthesis of heterogeneous cDNA according to the

manufacturer's instructions. The amplified RNA was labeled with biotin-16-UTP (Perkin Elmer Life and Analytical Sciences) in a 1:1 ratio with unlabeled UTP and was subsequently hybridized to a pilot version of the Illumina HumanRef-8 Beadchip (Illumina, Inc.). This array assays a total of 24,357 transcripts based on the database of the National Center for Biotechnology Information Reference Sequence (RefSeq database). Hybridized products were observed using Cy3-streptavidin (GE Healthcare Bio-Sciences) according to the BeadChip manual. Arrays were then scanned with an Illumina bead array confocal scanner and analyzed using Illumina Beadstudio software.

Myelinating cultures. Myelinating cultures were prepared as described previously [21,22]. Embryonic dorsal root ganglia (DRG) were prepared from E15 rat pups. After trypsinization, DRG neurons were plated on collagen-coated plastic dishes (Sigma-Aldrich). To eliminate endogenous SCs and fibroblasts, cultures were treated twice for 24 h with cytosine arabinoside (10 μM) and were subsequently maintained for 5 to 7 days in neurobasal medium (Invitrogen) supplemented with 1% (FBS; Hyclone), 2M L-Glutamine, 2% B27-serum-free supplement (Invitrogen), and 10 ng/mL nerve growth factor (NGF) (Sigma-Aldrich). In case of significant contamination with endogenous non-neuronal cells, cycles of cytosine arabinoside treatment were repeated until all glial cells were eliminated. For co-culture experiments, immortalized hSCs were seeded onto rat DRG neurons at a density of 10,000 cells per well on 24-well plates or 50,000 cells per well in 35 mm plastic dishes. To discriminate immortalized hSCs from residual rat SCs (rSCs), the immortalized hSCs were labeled with Hoechst stain (Sigma-Aldrich) at 1:10,000 dilution for 30 min at 37°C before seeding onto rat DRG neurons. In a subset of experiments, GFP-tagged immortalized hSCs were used. To initiate myelination, cell cultures were switched to myelination medium containing Eagle's medium with Earle's salts and 15% FBS, 10 ng/mL NGF and 50 μg/mL ascorbic acid (Sigma-Aldrich).

Evaluation of myelination and neuronal morphology. Cell cultures were prepared as described above and stained with anti-MBP antibody (SMI94, Sternberger monoclonals) to observe myelinated internodes. For myelin quantification, pictures from a total of 10 cultures were obtained from all areas of the culture dish in which myelination could be observed and the mean length and total length of all MBP-stained internodes were measured. Data were expressed as total length of myelinated internodes per well and mean length of myelinated internodes. For quantification of perikaryon diameter, cell cultures were stained with anti-neurofilament antibody and diameter of 20–30 perikarya in each cell culture was measured. The results from each culture were averaged and counted as $n = 1$ for statistical analysis. For quantification of neurite density, pictures were obtained from representative areas of the cell culture and neurofilament-positive neurites were quantified by fluorescence/pixel analysis.

Evaluation of SC proliferation in myelinating cultures. hSC-rat DRG co-cultures were prepared as described above and placed in myelinating media for 10 days. Then, cells were labeled with 10 μM Bromodeoxyuridine (BrdU; Sigma-Aldrich) for 4 h at 37°C. After fixation with Camoy's fixative buffer (3 parts methanol and 1 part acetic acid) at −20°C for 20 min, cells were denatured by adding 1 mL of 2N HCl in water and incubated at 37°C for 1 h. For immunostaining, cells were incubated in 0.2% Triton-X100 in phosphate-buffered saline (PBS) at room temperature for 10 min, and blocked with 5% normal goat serum in PBST (PBS plus Tween-20) at room temperature for 30 min. Co-cultured cells were subsequently incubated overnight at 4°C in anti-BrdU monoclonal antibody (Sigma-Aldrich; catalog no. B8434, at 1:500 dilution) and antineurofilament polyclonal antibody (Chemicon AB1982, at 1:500 dilution) diluted in 5% normal goat serum in PBST. FITC-conjugated goat anti-mouse IgG1 (Jackson ImmunoResearch Lab. Inc. catalog no. 115-095-205, at 1:1,000 dilution) was used to detect anti-BrdU antibody, whereas Texas Red-conjugated goat anti-rabbit IgG (Vector Labs, catalog no. TI 1000, at 1:1,000 dilution) was used to detect antineurofilament antibody.

ATP-based cytotoxicity assay. Immortalized hSCs were cultured in 96-well plates at a concentration of 10,000–20,000 cells/well. H_2O_2 was used as a toxic agent in different concentrations ranging from 0.15% to 0.75% with different incubation periods ranging from 1 up to 24 h. Cellular ATP levels were determined using the ViaLight Plus kit (Cambrex) according to manufacturer's instructions, as described previously [12].

Statistical analysis

For statistical analysis Student's *t*-test was used for variables with Gaussian distribution and Mann–Whitney *U* test for other variables. $P < 0.05$ was considered statistically significant.

Results

Immortalized hSCs express SC markers

The primary hSC cultures we used to generate the cell lines were more than 90% pure and were used within 2 weeks of establishing the cultures. From the primary hSC cultures, we generated multiple human fetal SC lines using the immortalization technique as described above. Using RT–PCR and immunostaining, we examined the expression profile of different glial markers in at least 3 separate SC lines. By immunostaining, nonmyelinating pure immortalized hSC cultures showed a positive staining for GFAP, p75, and S100β (Fig. 1A) but no staining for MBP (not shown). When appropriate controls with omission of primary or secondary antibodies were carried out, there was no nonspecific staining. At the mRNA level, immortalized hSCs expressed all tested markers with higher expression levels for the intermediate filament vimentin and the extracellular matrix (ECM) glycoprotein tenascin-C and lower levels for GFAP and S100β (Fig. 1B).

A detailed gene expression profile of immortalized hSCs

In a further attempt to characterize gene expression profile of immortalized hSCs, we used an Illumina microarray. In this array a total of 24,357 different transcripts were analyzed, including cell surface markers, growth factors, receptors, transcription factors, and molecules of the ECM. By using this approach, we identified a total of 3,508 different transcripts with high detection level compared with human oligodendrocytes precursors (Supple-

mentary Table 1; Supplementary Data are available online at www.liebertonline.com/scd) and 831 different transcripts with high detection level compared with human astrocyte cell lines (Supplementary Table 2). A selected list of genes categorized as transcription factors, growth factors, and receptors is shown in Table 1. In general, SC-specific markers such as transcription factors Slug (Gene symbol SNAI2), Hoxa2, S100A, ERBB3, and Integrin A4 (Gene symbol ITGA4), as well as neural crest markers expressed by SCs (Sox9, TWIST) were readily detected in the array [14]. Some markers, including p75 (Gene symbol NGFR) and Brn3a (Gene symbol Pou4F1), were not detected, which, based on our experience, might be due to the inefficient hybridization of samples with the probes that need to be improved or re-designed. To confirm this expression profile we chose a panel of 13 transcripts, of which we determined the relative expression in comparison to GAPDH by real-time RT–PCR. Based on the characteristic ability of SCs to synthesize components of ECM, we focused mainly on ECM proteins. All of the tested transcripts could be detected by qRT–PCR (Fig. 1C), with higher levels for collagen type IVα2, collagen type Vα1, tissue inhibitor of metalloproteinase 2, and α-Enolase (Fig. 1D).

Table 1. Important Pathways Identified in Human Schwann Cell Line as Compared with Fetal-Derived Human Oligodendrocyte Precursors

		Receptors		*Growth factors*	
Symbol	*hSC/hOPC*	*Symbol*	*hSC/hOPC*	*Symbol*	*hSC/hOPC*
Transcription factors					
CART1	117.8	ANTXR1	20.0	BDNF	37.3
DUX2	24.1	BDKRB1	123.7	BGN	100.9
ETS2	57.2	CHRNB2	2.3	CCL20	106.5
HOXA3	24.8	CMKLR1	32.9	CKLFSF7	7.1
IPF1	50.6	DRD1	6.9	CRHBP	5.3
MLLT7	3.0	EPOR	126.7	CSF2	73.5
PAX8	5.9	ERBB2	52.4	CXCL2	3.7
PITX2	20.1	FN5	33.0	IGFBP3	7.6
PRDM1	7.7	GPR107	4.4	IGFBP4	30.0
RORC	34.5	GPR108	2.5	IGFBP6	33.1
SNAI2	5.9	GPR160	267.9	IL11	6.8
TBX3	59.0	GPR87	30.1	IL1A	40.0
TCF21	11.4	GRIN2D	3.5	IL1B	840.5
TGIF	2.5	HTR7	36.0	IL6	951.1
TLX2	2.7	IGF1R	2.5	INHBA	33.1
TWIST2	346.7	IL1R2	31.8	INHBE	74.4
		KLRD1	5.0	LIF	9.9
Cell surface markers		OSMR	129.6	TNFSF12	35.3
ACE	3.3	P2RY10	31.0	VEGFC	28.3
ACTA2	5.9	PPFIA1	2.6	WNT5A	18.4
ANPEP	811.2	RARB	405.6		
COL1A2	7.1	RIPK1	3.8		
COL3A1	370.3	RORC	34.5		
DPP4	3.5	TNFRSF10A	57.2		
ENG	533.2	TNFRSF11A	50.5		
IL1R2	31.8	TNFRSF8	4.7		
ITGA1	54.8	TNFRSF9	3.5		
KLRD1	5.0				
SERPINE1	39.3				
TNFRSF8	4.7				

hSC/hOPC represents the ratio of the signal values detected for hSC and hOPC. Schwann cell-specific transcription factors TWIST and SLUG (SNAI2) were expressed at high levels together with several cell surface markers, receptors, and growth factors. hSC, human Schwann cell line; hOPC, human oligodendrocyte precursors.

Immortalized human fetal SCs myelinate rat sensory axons in vitro

To determine if immortalized hSCs retain their ability to myelinate peripheral axons in vitro, we prelabeled human immortalized SCs with Hoechst stain and added them to established cultures of rat embryonic DRG sensory neurons. After 3 weeks in culture, hSCs had ensheathed bundles of sensory axons and myelin segments could be observed with anti-MBP staining (Fig. 2A–D). An analysis of single myelin segments confirmed that hSCs and not residual contaminating rat glial cells were the myelin forming cells as revealed by the prelabeled (blue-colored) SC nuclei (Fig. 2C, D).

In further experiments we compared the efficacy of human and rSCs to myelinate embryonic rat DRG neurons. In side-by-side experiments embryonic rat DRG neurons were cultured with endogenous rSCs or with immortalized hSCs after treatment with AraC. After 21 days, all cell cultures with rSCs displayed MBP-positive myelinated internodes (Fig. 3). In contrast, the number of myelinated internodes in cell cultures of immortalized hSCs was 100-fold less in comparison to rSCs, suggesting a markedly reduced efficacy of immortalized hSCs to myelinate rat sensory neurons. Further, the average length of MBP-positive internodes was significantly shorter in DRG cultures with immortalized hSCs (Fig. 3B, C). An analysis of the morphology of rat DRG neurons co-cultured with either rat or immortalized hSCs further revealed that neurons that were co-cultured with immortalized hSCs had a significant smaller perikaryon diameter and a reduced neurite network (Fig. 4).

Immortalized human fetal SCs retain susceptibility to oxidative stress

To test their utility for drug-screening assays, immortalized hSCs were treated with H_2O_2, an oxidant that is known to induce cell lysis by pathways that include the activation of poly(ADP-ribose) polymerase and subsequent loss of ATP [23]. Similar to primary human or rodent glial cells [24], H_2O_2 induced a marked cell lysis of immortalized hSCs at fairly low concentrations (Fig. 5A) and within 1 h after incubation with H_2O_2 (Fig. 5B). These results underline that after immortalization SCs remain sensitive to H_2O_2-induced cell lysis.

Discussion

In the present study, we generated several immortalized hSC lines that retain characteristics of primary SCs, including expression of glial cell markers and components of the ECM, and ability to myelinate rodent sensory neurons.

The ability of SCs to promote peripheral nerve regeneration has led to intensive research about their potential use for

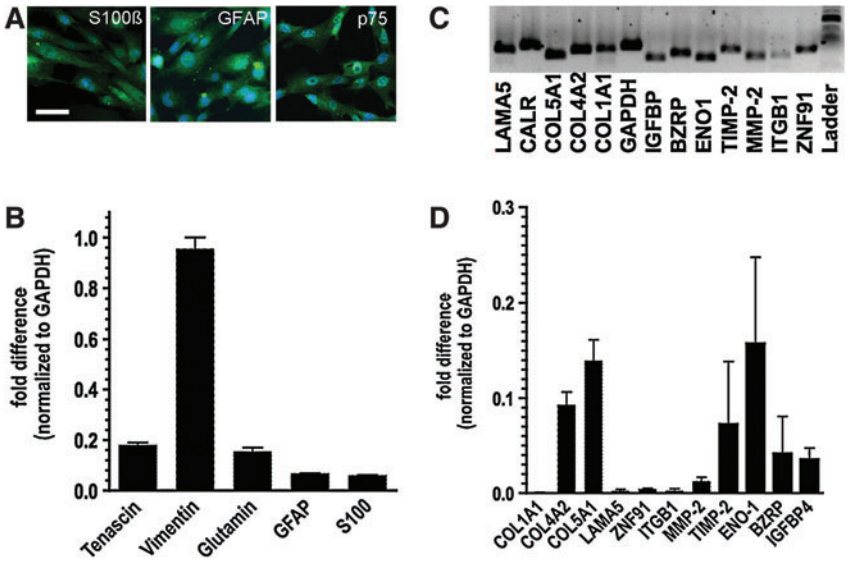

FIG. 1. **(A)** Immunofluorescence images of immortalized nonmyelinating pure Schwann cells stained positive with antibodies against S100β, GFAP, and p75 (bar = 100 μm). Nuclei are counterstained with DAPI (*blue color*). **(B)** Immortalized human Schwann cells express mRNA for different Schwann cell markers as determined by real-time RT–PCR. **(C,D)** Gene product and quantitative mRNA expression of 11 transcripts, which were previously detected by microarray were reconfirmed by real-time PCR. ENO1, α-enolase 1; ZNF91, zinc finger protein 91; IGFBP4, insulin-like growth factor-binding protein 4; BZRP, benzodiazapine receptor; ITGB1, integrin beta 1; COL4A2, collagen type IVα2; COL5A1, collagen type Vα1; COL1A1, collagen type Iα1; MMP-2, matrix metalloproteinase-2; CALR, calreticulin; LAMA5, laminin α5 (LAMA5); TIMP-2, tissue inhibitor of metalloproteinase-2. RT–PCR, reverse transcription–polymerase chain reaction; GFAP, glial fibrillary acidic protein; DAPI, 4′,6-diamidino-2-phenylindole. Color images available online at www.liebertonline.com/scd

cell transplantation to support regeneration in the PNS and central nervous system (CNS). Indeed, SCs have been shown to promote axonal regeneration and remyelinate regrowing axons in various experimental paradigms of CNS and PNS injury [3,25–27]. These studies support the idea that in humans, after nerve injury, autologous SCs could be obtained from healthy nerves, expanded ex vivo, and retransplanted at the sites of injury [28,29].

However, SC auto-transplantation paradigm in humans has not been systematically pursued over the years and is still far from being introduced in clinical practice. One of the reasons is that function of SCs has been mostly studied in

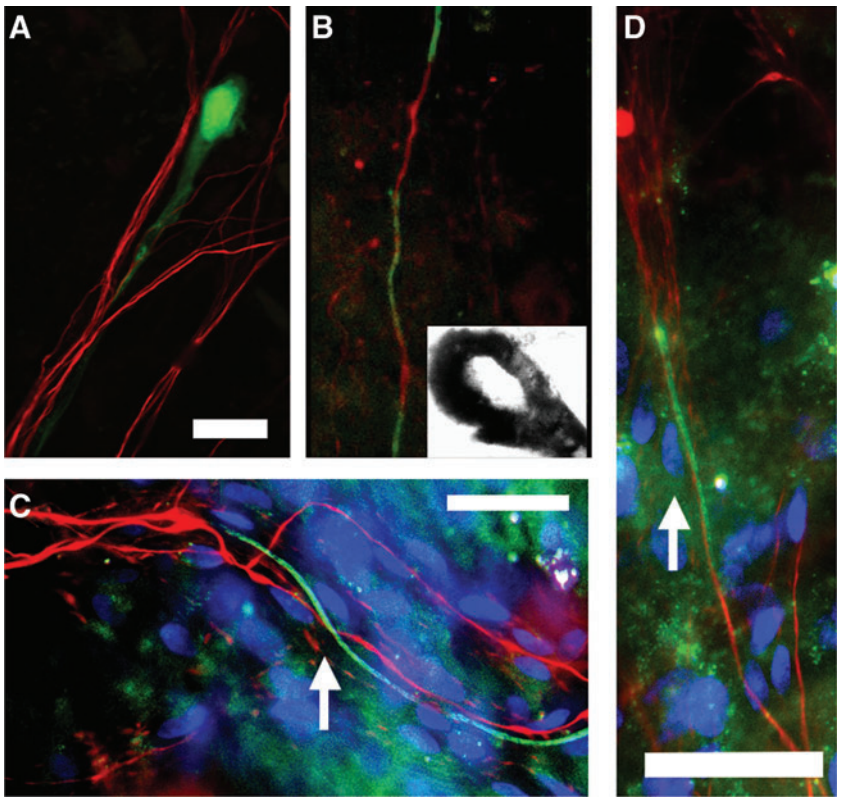

FIG. 2. **(A)** In co-culture, green fluorescent protein-labeled human Schwann cells elongate and become closely attached to rat sensory axons (stained *red* with anti-neurofilament antibody, bar = 20 μm). **(B)** In vitro myelination in co-cultures of human Schwann cells and DRG neurons confirmed by staining against MBP (*green*) and electron microscopy (*inset*). **(C, D)** Co-cultures of human Schwann cells and rat sensory neurons. Schwann cells, which are prelabeled with Hoechst stain (*blue*), have ensheathed rat axons (*red* = neurofilament stainig) and some of the human Schwann cells form single myelin segments (*green* = anti-MBP staining, *arrow* = nucleus of human myelinating Schwann cell, bar = 100 μm). DRG, dorsal root ganglia; MBP, myelin basic protein. Color images available online at www.liebertonline.com/scd

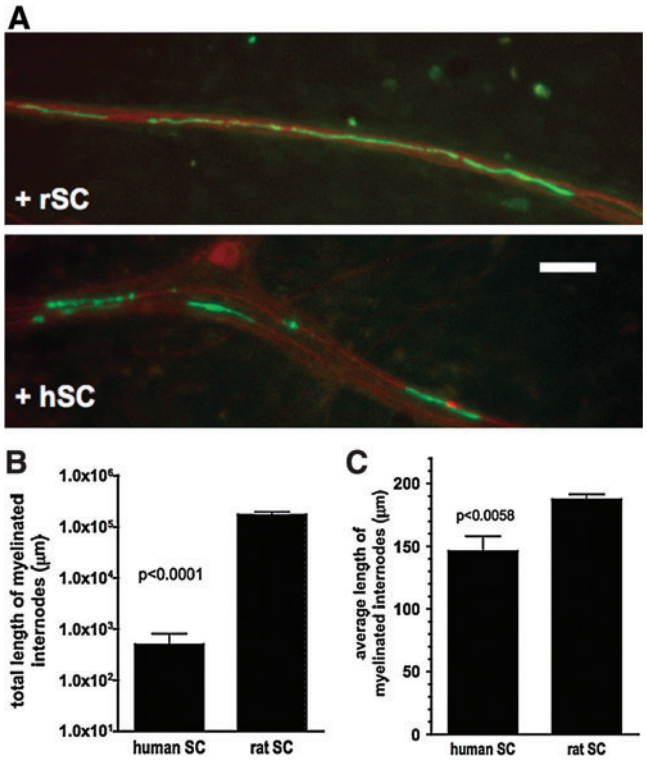

FIG. 3. Comparison of rat neuron–human Schwann cell co-cultures and rat neuron–rat Schwann cell co-cultures. **(A)** Immunofluorescence of co-cultures with rat (+rSC) and human Schwann cells (+hSC) stained with antineurofilament antibody (*red*) and anti-MBP antibody (*green*, bar = 100 µm). **(B)** Quantification of the total length of myelinated internodes. Human Schwann cells form much fewer myelinated internodes than rat Schwann cells. **(C)** Quantification of the average length of myelinated internodes. Human Schwann cells form shorter myelinated internodes in comparison to rat Schwann cells. Color images available online at www.liebertonline.com/scd

rodent models, which make it difficult to extrapolate the results to humans. In addition, SCs obtained from human donors are difficult to maintain in cell culture; low yields and poor proliferation rate result in overgrowth by fibroblasts [16–18,30]. As a consequence, only intricate, time-consuming purification and expansion procedures allow establishing primary hSCs cultures in low numbers to study their functional characteristics [16,17,31]. Procedures that have been proposed to increase purity and yield of harvested hSCs include magnetic-activated cell separation [32], addition of growth and differentiation factors (neuregulin/forskolin) [13], as well as modulation of signaling pathways such as extracellular signal-regulated kinase Erk1 and Erk2 [15].

We sought to overcome drawbacks associated with culturing hSCs by generating a cell line that retains the properties of a primary hSC yet is easy to grow and propagate. By immortalizing fetal hSCs we were able to generate cell lines that meet these criteria. Since the essential function of SCs is their ability to myelinate axons, we further assessed the potential of our cell lines to myelinate rat sensory axons in vitro. Using similar in vitro models, it has been shown previously that embryonic and adult hSCs are able to myelinate rat axons [17,18]. However, the amount of myelin is generally much less abundant compared with co-cultures with rSCs. In those studies, adult or embryonic hSCs were co-cultured with rat or human sensory neurons, which led to a sporadic myelination of solitary neurons. It has been suggested that hSCs may have negative effect on the health of neurons in this cell culture system, based on observations that the addition of human SC to neurons, regardless of human or rat, led to shrinkage of neuronal cell bodies and to a progressive loss of neurites [17,18].

Consistent with those observations, our immortalized hSCs were able to myelinate rat axons; however, the amount of myelination was 100-fold less in comparison to cell culture-containing neonatal rSCs. Given the fact that 10,000 cells were initially added to the culture dish, <0.1% of SCs

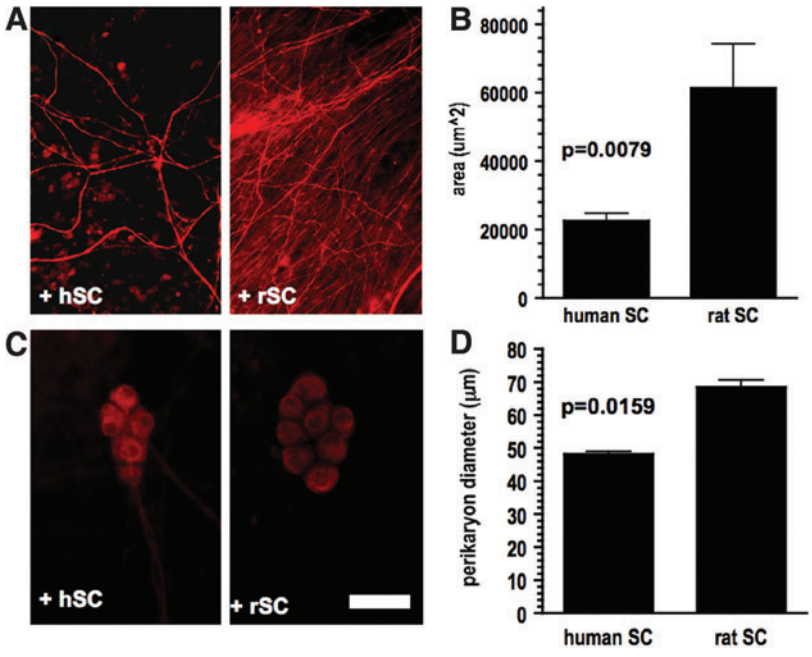

FIG. 4. Comparison of the neuron morphology of rat sensory neurons cultured with either human or rat Schwann cells. **(A)** Neurofilament staining of co-cultures with rat (+rSC) or human Schwann cells (+hSC) revealed a reduced neurite density in cultures with human Schwann cells. **(B)** Quantification of the neurite density of co-cultures with either rat or human Schwann cells. **(C)** Rat neurons that are co-cultured with human Schwann cells reveal smaller, shrunken perikarya (bar = 100 µm). **(D)** Quantification of the average perikaryon diameter of rat neurons cultured with either rat or human Schwann cells. Color images available online at www.liebertonline.com/scd

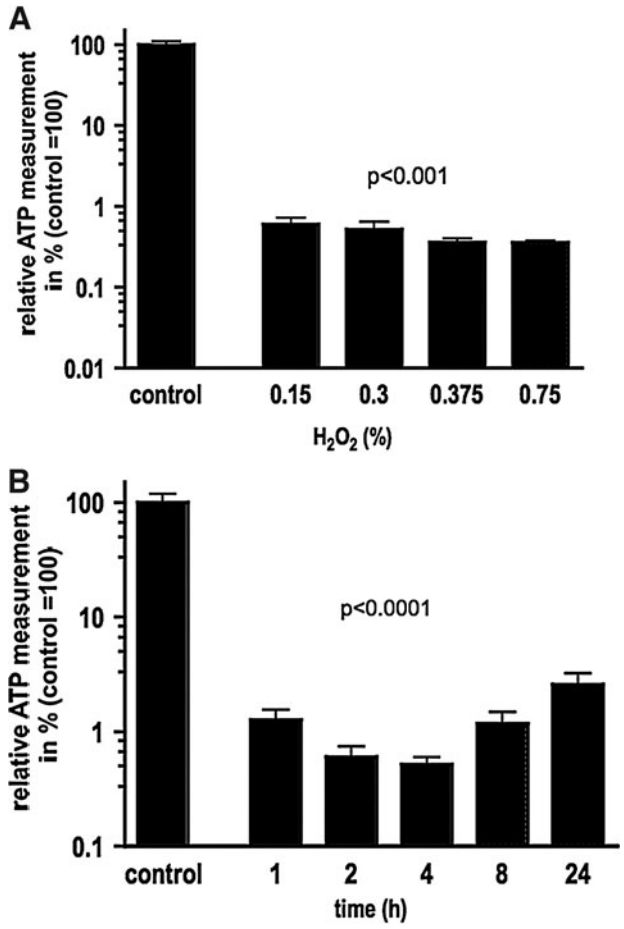

FIG. 5. Immortalized human fetal Schwann cells show marked susceptibility to oxidative stress induced by H_2O_2. **(A)** Treatment of Schwann cells with different concentrations of H_2O_2 lead to a marked cell lysis as determined by ATP measurement. **(B)** Different incubation periods of Schwann cells with 0.375% H_2O_2 demonstrates an effect of H_2O_2 within 1 h after incubation.

change to a myelinating phenotype. This, nevertheless, showed that our immortalization procedure did not inhibit the ability of cells to differentiate. One could argue that the low myelination potential is because the majority of SCs are unable to exit the cell cycle and continue to proliferate. However, since we did not observe any overgrowth of SCs in our co-culture system, we conclude that the immortalized SCs stop dividing when cultured in differentiation media and start to differentiate into nonmyelinating (majority) and myelinating (minority) phenotypes. Further, when assessed for proliferation capacity, hSCs had a marked decrease in BrdU incorporation when cultured with rat DRG neurons in myelinating media (Supplementary Fig. 1). Further experiments would be needed to determine if changes in cell culture conditions could enhance the myelination by immortalized hSCs. However, the similarity between our results and from those studies with primary SCs favor the hypothesis that the intrinsic capacity of hSCs in this cell culture model is generally lower than those of the rSCs. In addition, when we compared the morphology of neurons cultured with either immortalized hSCs or rSCs, it turned out that the neurite density in cultures with hSCs was strikingly reduced and the average neuronal cell body diameter was significantly lower than those cultures with rSCs. These results confirm the published observations that human and rSCs have very divergent effects on rodent sensory neuronal health in vitro and may provide an explanation for the poor capability of immortalized hSCs to myelinate neurons in vitro.

Apart from studying myelination in vitro, immortalized cell lines may represent a useful tool for high-throughput drug screening to identify compounds that maybe therapeutically useful in peripheral neuropathies in which SC dysfunction plays a role in pathogenesis. Compared with rSC lines used for this purpose, immortalized hSC lines we developed likely offer an advantage as they may represent characteristics of the human primary SCs better. Further, unlike primary cells isolated from different sources, homogeneity of the immortalized hSCs is a major advantage to reduce well-to-well variability in high-throughput drug screening.

Since primary SCs are susceptible to apoptosis caused by H_2O_2 and, on the other hand, hTERT expression vectors could theoretically affect the response of these cells exposed to oxidative stress, we explored the utility of immortalized hSCs as a tool in high-throughput assays and developed a simple toxicity assay. Using a luciferase-based assay, we measured cellular ATP levels, which strongly correlate with the number of healthy cells [12,33]. The advantage of the luciferase-based assay is that it is suitable for scaling up for high-throughput robotic assays because it does not involve any washing step, which often induces variability in such assays. As a proof-of-concept assay we chose to assess toxicity of H_2O_2. Although short-term application of H_2O_2 may not fully replicate the slow, progressive oxidative stress that is seen in vivo, it has been used to model oxidative stress in a variety of degenerative and inflammatory diseases of the nervous system [34–37]. Future studies can be directed at in vitro models that mimic pathogenic mechanisms in which SC pathology plays a role; for example, high glucose exposure can be used to mimic diabetes or reporter assays can be developed to enhance *pmp22* gene expression in hereditary neuropathy with liability to pressure palsies.

The gene expression dataset generated from the immortalized hSC line will serve as a useful baseline for comparative studies for other types of immortalized cell lines and cells generated from stem cell populations [38–42]. Highly expressed genes are listed in Supplementary Tables 1 and 2, and the entire set of expressed genes is available upon request. Comparison of the gene expression profile of the hSC to human oligodendrocyte precursors or astrocytes reveals that although there are many similarities, key differences remain. Expression profile of genes unique to SCs can be used to validate cells generated from stem cells before widespread use in mechanistic or drug discovery studies.

In summary, we have developed several immortalized hSC lines, which show essential characteristics of primary hSCs, including their ability to myelinate. Our study supports the notion that immortalization techniques can be useful to generate human cell lines from cells that are considered difficult to immortalize such as SCs. In contrast to primary cell cultures, these cells tolerate easy cell culture conditions, which allow establishment of simple, time and cost efficient in vitro assays to screen large numbers of compounds for potential therapeutic use.

Acknowledgments

This work was supported by grants from NIH (R01-NS43991) and Adelson Medical Research Foundation. H.C.L. is supported by a grant from the German research foundation (DFG, Le2368-1/1). We thank Hong Liang and Chunhua Zhou for technical assistance.

Author Disclosure Statement

No competing financial interests exist.

References

1. Friedman B, SS Scherer, JS Rudge, M Helgren, D Morrisey, J McClain, DY Wang, SJ Wiegand, ME Furth, RM Lindsay et al. (1992). Regulation of ciliary neurotrophic factor expression in myelin-related Schwann cells *in vivo*. Neuron 9:295–305.
2. Acheson A, PA Barker, RF Alderson, FD Miller and RA Murphy. (1991). Detection of brain-derived neurotrophic factor-like activity in fibroblasts and Schwann cells: inhibition by antibodies to NGF. Neuron 7:265–275.
3. Levi AD and RP Bunge. (1994). Studies of myelin formation after transplantation of human Schwann cells into the severe combined immunodeficient mouse. Exp Neurol 130:41–52.
4. Heumann R, S Korsching, C Bandtlow and H Thoenen. (1987). Changes of nerve growth factor synthesis in non-neuronal cells in response to sciatic nerve transection. J Cell Biol 104:1623–1631.
5. Court FA, L Wrabetz and ML Feltri. (2006). Basal lamina: Schwann cells wrap to the rhythm of space-time. Curr Opin Neurobiol 16:501–507.
6. Keswani SC, U Buldanlioglu, A Fischer, N Reed, M Polley, H Liang, C Zhou, C Jack, GJ Leitz and A Hoke. (2004). A novel endogenous erythropoietin mediated pathway prevents axonal degeneration. Ann Neurol 56:815–826.
7. Jessen KR and R Mirsky. (2008). Negative regulation of myelination: relevance for development, injury, and demyelinating disease. Glia 56:1552–1565.
8. Weishaupt A, W Bruck, T Hartung, KV Toyka and R Gold. (2001). Schwann cell apoptosis in experimental autoimmune neuritis of the Lewis rat and the functional role of tumor necrosis factor-alpha. Neurosci Lett 306:77–80.
9. Lehmann HC, A Kohne, G Meyer zu Horste, T Dehmel, O Kiehl, HP Hartung, S Kastenbauer and BC Kieseier. (2007). Role of nitric oxide as mediator of nerve injury in inflammatory neuropathies. J Neuropathol Exp Neurol 66:305–312.
10. Hafer-Macko CE, KA Sheikh, CY Li, TW Ho, DR Cornblath, GM McKhann, AK Asbury and JW Griffin. (1996). Immune attack on the Schwann cell surface in acute inflammatory demyelinating polyneuropathy. Ann Neurol 39:625–635.
11. Hoke A. (2006). Mechanisms of Disease: what factors limit the success of peripheral nerve regeneration in humans? Nat Clin Pract Neurol 2:448–454.
12. Chen W, R Mi, N Haughey, M Oz and A Hoke. (2007). Immortalization and characterization of a nociceptive dorsal root ganglion sensory neuronal line. J Peripher Nerv Syst 12:121–130.
13. Casella GT, RP Bunge and PM Wood. (1996). Improved method for harvesting human Schwann cells from mature peripheral nerve and expansion *in vitro*. Glia 17:327–338.
14. Miller SJ, F Rangwala, J Williams, P Ackerman, S Kong, AG Jegga, S Kaiser, BJ Aronow, S Frahm, et al. (2006). Large-scale molecular comparison of human schwann cells to malignant peripheral nerve sheath tumor cell lines and tissues. Cancer Res 66:2584–2591.
15. Tapinos N and A Rambukkana. (2005). Insights into regulation of human Schwann cell proliferation by Erk1/2 via a MEK-independent and p56Lck-dependent pathway from leprosy bacilli. Proc Natl Acad Sci USA 102:9188–9193.
16. Rutkowski JL, CJ Kirk, MA Lerner and GI Tennekoon. (1995). Purification and expansion of human Schwann cells *in vitro*. Nat Med 1:80–83.
17. Morrissey TK, N Kleitman and RP Bunge. (1995). Human Schwann cells *in vitro*. II. Myelination of sensory axons following extensive purification and heregulin-induced expansion. J Neurobiol 28:190–201.
18. Morrissey TK, RP Bunge and N Kleitman. (1995). Human Schwann cells *in vitro*. I. Failure to differentiate and support neuronal health under co-culture conditions that promote full function of rodent cells. J Neurobiol 28:171–189.
19. Brockes JP, KL Fields and MC Raff. (1979). Studies on cultured rat Schwann cells. I. Establishment of purified populations from cultures of peripheral nerve. Brain Res 165:105–118.
20. van Gelder RN, ME von Zastrow, A Yool, WC Dement, JD Barchas and JH Eberwine. (1990). Amplified RNA synthesized from limited quantities of heterogenous cDNA. Proc Natl Acad Sci USA 87:1663–1667.
21. Podratz JL, E Rodriguez and AJ Windebank. (2001). Role of the extracellular matrix in myelination of peripheral nerve. Glia 35:35–40.
22. Lehmann HC, A Kohne, F Bernal, P Jangouk, G Meyer Zu Horste, T Dehmel, HP Hartung, SC Previtali and BC Kieseier. (2009). Matrix metalloproteinase-2 is involved in myelination of dorsal root ganglia neurons. Glia 57:479–489.
23. Schraufstatter IU, DB Hinshaw, PA Hyslop, RG Spragg and CG Cochrane. (1986). Oxidant injury of cells. DNA strand-breaks activate polyadenosine diphosphate-ribose polymerase and lead to depletion of nicotinamide adenine dinucleotide. J Clin Invest 77:1312–1320.
24. Heine S, J Ebnet, S Maysami and M Stangel. (2006). Effects of interferon-beta on oligodendroglial cells. J Neuroimmunol 177:173–180.
25. Golden KL, DD Pearse, B Blits, MS Garg, M Oudega, PM Wood and MB Bunge. (2007). Transduced Schwann cells promote axon growth and myelination after spinal cord injury. Exp Neurol 207:203–217.
26. Pearse DD, AR Sanchez, FC Pereira, CM Andrade, R Puzis, Y Pressman, K Golden, BM Kitay, B Blits, PM Wood and MB Bunge. (2007). Transplantation of Schwann cells and/or olfactory ensheathing glia into the contused spinal cord: Survival, migration, axon association, and functional recovery. Glia 55:976–1000.
27. Levi AD, V Guenard, P Aebischer and RP Bunge. (1994). The functional characteristics of Schwann cells cultured from human peripheral nerve after transplantation into a gap within the rat sciatic nerve. J Neurosci 14:1309–1319.
28. Guest JD, A Rao, L Olson, MB Bunge and RP Bunge. (1997). The ability of human Schwann cell grafts to promote regeneration in the transected nude rat spinal cord. Exp Neurol 148:502–522.
29. Hill CE, LD Moon, PM Wood and MB Bunge. (2006). Labeled Schwann cell transplantation: cell loss, host Schwann cell replacement, and strategies to enhance survival. Glia 53:338–343.
30. Levi AD, PJ Evans, SE Mackinnon and RP Bunge. (1994). Cold storage of peripheral nerves: an *in vitro* assay of cell viability and function. Glia 10:121–131.

31. Morrissey TK, AD Levi, A Nuijens, MX Sliwkowski and RP Bunge. (1995). Axon-induced mitogenesis of human Schwann cells involves heregulin and p185erbB2. Proc Natl Acad Sci USA 92:1431–1435.
32. Vroemen M and N Weidner. (2003). Purification of Schwann cells by selection of p75 low affinity nerve growth factor receptor expressing cells from adult peripheral nerve. J Neurosci Methods 124:135–143.
33. Crouch SP, R Kozlowski, KJ Slater and J Fletcher. (1993). The use of ATP bioluminescence as a measure of cell proliferation and cytotoxicity. J Immunol Methods 160:81–88.
34. White AR, H Zheng, D Galatis, F Maher, L Hesse, G Multhaup, K Beyreuther, CL Masters and R Cappai. (1998). Survival of cultured neurons from amyloid precursor protein knock-out mice against Alzheimer's amyloid-beta toxicity and oxidative stress. J Neurosci 18:6207–6217.
35. Lezoualc'h F, Y Sagara, F Holsboer and C Behl. (1998). High constitutive NF-kappaB activity mediates resistance to oxidative stress in neuronal cells. J Neurosci 18:3224–3232.
36. Desagher S, J Glowinski and J Premont. (1997). Pyruvate protects neurons against hydrogen peroxide-induced toxicity. J Neurosci 17:9060–9067.
37. Nicholls DG. (2004). Mitochondrial dysfunction and glutamate excitotoxicity studied in primary neuronal cultures. Curr Mol Med 4:149–177.
38. Lee G, SM Chambers, MJ Tomishima and L Studer. Derivation of neural crest cells from human pluripotent stem cells. Nat Protoc 5:688–701.
39. El Seady R, MA Huisman, CW Lowik and JH Frijns. (2008). Uncomplicated differentiation of stem cells into bipolar neurons and myelinating glia. Biochem Biophys Res Commun 376:358–362.
40. Lee G, H Kim, Y Elkabetz, G Al Shamy, G Panagiotakos, T Barberi, V Tabar and L Studer. (2007). Isolation and directed differentiation of neural crest stem cells derived from human embryonic stem cells. Nat Biotechnol 25:1468–1475.
41. Li HY, EH Say and XF Zhou. (2007). Isolation and characterization of neural crest progenitors from adult dorsal root ganglia. Stem Cells 25:2053–2065.
42. McKenzie IA, J Biernaskie, JG Toma, R Midha and FD Miller. (2006). Skin-derived precursors generate myelinating Schwann cells for the injured and dysmyelinated nervous system. J Neurosci 26:6651–6660.

Address correspondence to:
Dr. Ahmet Höke
Department of Neurology
Johns Hopkins University School of Medicine
855 N. Wolfe Street
Rangos 248
Baltimore, MD 21205

E-mail: ahoke@jhmi.edu

Received for publication November 15, 2010
Accepted after revision May 16, 2011
Prepublished on Liebert Instant Online May 17, 2011